



# Hydrological and hydraulic drivers of microplastics in a rural river sourced from the UK's largest opencast coal mine<sup>☆</sup>

James Lofty<sup>a,\*</sup>, Guglielmo Sonnino Sorisio<sup>a</sup>, Liam Kelleher<sup>b,c</sup>, Stefan Krause<sup>b,c,d</sup>, Pablo Ouro<sup>e</sup>, Catherine Wilson<sup>a</sup>

<sup>a</sup> Cardiff University, School of Engineering, Hydro-Environmental Research Centre, Cardiff, Wales, UK

<sup>b</sup> University of Birmingham, School of Geography, Earth and Environmental Sciences, Birmingham, England, UK

<sup>c</sup> Birmingham Institute of Sustainability and Climate Action, Birmingham, England, UK

<sup>d</sup> LEHNA (Laboratoire d'Ecologie des Hydrosystèmes Naturels et Anthropisés), University of Lyon, Villeurbanne, France

<sup>e</sup> University of Manchester, Department of Civil Engineering and Management, School of Engineering, Manchester, UK

## ARTICLE INFO

### Keywords:

Microplastic in rivers  
Coal mining pollution  
Freshwater resources  
Rainfall-runoff  
Total suspended sediments

## ABSTRACT

Microplastics (MPs) are ubiquitous in river and freshwater ecosystems. However, the hydraulic and hydrological mechanisms that regulate the activation and emissions of MPs from both the land surface and subsurface into rivers are not well understood. This study aims to quantify the instream MP concentration and MP load in a remote headwater catchment river (Taff Bargoed, Wales, UK), which drains the UK's largest opencast coal mine (Ffos-y-fran), over a two-year period. Small fibers (< 1 mm) composed of acrylic and polyester dominated the MPs found in the Taff Bargoed, while less commonly observed MP fragments were mostly composed of poly-sulfone. River MP concentrations ranged from 0.27 to 28.87 MP/m<sup>3</sup> (average: 14.60 ± 10.31 MP/m<sup>3</sup>), and MP load ranged one order of magnitude from 0.08 to 3.04 MP/s (average: 1.42 ± 0.81 MP/s). Statistically significant relationships were found between MP concentration, the number of dry weather hours and river discharge, which indicated rainfall-runoff induced, source limited, dilution effects on instream MP concentration. A negligible relationship between MP load and river discharge was observed, which suggests that MP load variability was independent of flow conditions, dry weather hours, and the MP concentration in the Taff Bargoed. Significant positive relationships between MP concentration and instream total suspended solids were also observed, indicating that this may provide a useful proxy for estimating MP variation in the Taff Bargoed. No longitudinal variation in MP concentration over a 2 km reach was observed, where differences in flow and drainage area were negligible, however, MP concentration increased by a factor of 2–4 downstream of an inflowing tributary, also sourced from the Ffos-y-fran coal mine. Overall, the results of this study provide evidence that mining activities can contribute MPs in rural and remote rivers, with their contribution being regulated by the hydraulic and hydrological processes in the catchment.

## 1. Introduction

Rivers are major conveyors of highly hazardous microplastic (MP) pollution particles (plastics <5 mm in size) (Mai et al., 2020; González-Fernández et al., 2023; Stokal et al., 2023). There is increasing evidence that in river environments MPs may pose threats to biodiversity, food security and freshwater resources (Krause et al., 2021; MacLeod et al., 2021; Nava et al., 2023). More concerning is the growing evidence of the potential harm caused by MPs to human health (Dick

Vethaak and Legler, 2021; Krause et al., 2024) with plastics being discovered in human lung tissue (Jenner et al., 2022), the placenta (Amereh et al., 2022; Ragusa et al., 2022) and blood (Baas et al., 2022; Leslie et al., 2022). This confirms that MPs from the environment can enter the human body through multiple pathways, such as inhalation and ingestion, including through drinking water (Krause et al., 2024). These potential threats posed by MPs have caused a transgression of a planetary boundary, indicating that the Earth's planetary limits for MP pollution have been exceeded (Persson et al., 2022).

<sup>☆</sup> This paper has been recommended for acceptance by Eddy Y. Zeng.

\* Corresponding author.

E-mail address: [LoftyJ@cardiff.ac.uk](mailto:LoftyJ@cardiff.ac.uk) (J. Lofty).

The terrestrial environment has been identified as an important sink of MPs (Nizzetto et al., 2016; Lofty et al., 2022) and a source of MP pollution in rivers (Crossman et al., 2020; Han et al., 2022). Land use, whether rural or urban, has been linked to spatial and temporal variation of instream MP concentration (number of MPs per volume of water) and MP load (number of MPs transported per unit time) (Wagner et al., 2019; Kukkola et al., 2023). Typically, rivers in densely populated urban areas contain higher concentrations of MPs, due to the density of multiple diffuse (e.g. littering, roads, tyre wear, industrial processes, urban drainage) and point sources (e.g. wastewater treatment plants and combined sewer overflows) of MP pollution (Grbić et al., 2020; Kukkola et al., 2023; Kunz et al., 2023). However, the causation for correlations between the degree of urbanisation and riverine MP concentration is not always clear (Wagner et al., 2019; Kukkola et al., 2023), as rural and remote areas can also be significant sources for terrestrial MPs through littering due to tourism, breakdown of plastic mulch used in agriculture, use of sewage sludge as fertiliser and industrial processes (Qi et al., 2018; Feng et al., 2020; Huang et al., 2020; Lofty et al., 2022; Brožová et al., 2023).

Riverine MP concentration and MP load are highly variable and, to a large degree, driven by rainfall events, which potentially can activate and mobilise land-based MPs into rivers (Han et al., 2022; Cho et al., 2023; Kukkola et al., 2024). Previous studies have examined the relationship between rainfall-runoff and instream MP concentration and MP load, however, the MP rainfall-runoff response is complex and contrasting conclusions between studies have been drawn (Barrows et al., 2018; Wagner et al., 2019; Kurki-Fox et al., 2023; Moses et al., 2023). This variability can be attributed to source and transport limitations. For example, if MP concentration increases with increasing discharge, this indicates that the source of MP is active and proportionally supplying MPs to the river (transport limitation). This subsequently may increase MP load, as more MPs are being transported with larger discharges. On the other hand, if MP concentration decreases with increasing rainfall and river discharge, this means the emission of MPs from different sources is limited and cannot keep up with the increase in effective rainfall, leading to a dilution effect of MP concentration in the river (source limitation). The influence source limitation has on MP load is more complex because even if MP concentration decreases with increasing discharge, MP load may still increase because a higher discharge may be able to transport more MPs overall (Kukkola et al., 2023).

Coal mining is an industry that may generate and emit MP pollution into the surrounding environment through various pathways, including waste generated by tyre wear in transportation, land filling of opencasts with sewage sludge and mismanaged waste (Sipe et al., 2022; Brožová et al., 2023; Pinlova and Nowack, 2024). Coal mining also creates new drainage channels and exposes existing geological fractures, leading to the leaching of mining wastewater that can contain heavy metals, sediments, and potentially MP, which can then enter the surrounding surface water and groundwater (Zhu et al., 2022; Brožová et al., 2023). Despite industrial areas being a known source of MP pollution (Mani et al., 2015; Tibbetts et al., 2018; Woodward et al., 2021), only one study to date has quantified the MP emissions from an area of opencast coal mining into the surrounding groundwater (Brožová et al., 2023). However, the study did not focus on the contribution of MPs from the coal mining area into the surface water river network or provide a description of the hydraulic and hydrological processes which regulate the riverine MP variation. This is important in order to understand the discrete sources of MPs in remote and rural environments with industry.

This study aims to quantify the instream MP concentration and MP load in a rural headwater river (Taff Bargoed, South Wales, 0–0.1 people/km<sup>2</sup>, 450 m AMSL), which drains the UK's largest opencast coal mine (Ffos-y-fran, Wales), to assess the complex relationships between different terrestrial MP supplies (from the coal mine and surrounding rural environment) and the resultant riverine MP concentration and MP load. To achieve this, instream MP sampling of the Taff Bargoed is

conducted at five sampling sites along a remote longitudinal 2 km reach over a two-year period. Reach-scale longitudinal MP flux is described, as well as relationships between MP concentration, MP load, river discharge, the number of dry weather hours, and total suspended solids (TSS) to describe the hydraulic and hydrological processes that regulate instream MPs in a river fed from a large opencast coal mine.

## 2. Methods

### 2.1. Study area

The study was conducted at five sampling sites along a 2 km stretch of the upper reaches of the Taff Bargoed, located in Merthyr Tydfil, South Wales, UK. The study site was chosen because of its different land usages (industrial and unmanaged heathland), which provides a unique setting to investigate the sources and transport of MP in a mixed-use rural headwater river. Fig. 1A provides an overview of the study area, including the Ffos-y-fran opencast coal mine, while Fig. 1B–F shows a full characterisation of the study area conducted on ArcGIS, including a supervised land classification (Fig. 1B), land elevation (Fig. 1C), slope (Fig. 1D), and contributing catchment areas for each MP sampling site (Fig. 1E), following a protocol for MP field sampling proposed by (Lofty et al., 2023). Fig. 1G and H shows photographs of MP sampling sites on the Taff Bargoed.

The five sampling sites on the Taff Bargoed drain contributing catchment areas ranging between 1.48 km<sup>2</sup>–4.83 km<sup>2</sup> (Fig. 1E). The study area is rural, with the following land cover mix: 51% unmanaged heathland, 42% mining activity, 3% tree cover, 2% managed grassland and 2% industry (Fig. 1B). The Taff Bargoed catchment has a population density of 0–0.1 people/km<sup>2</sup> (Digimaps, 2024) and suspected sources of plastic pollution in the area include mining activities, transportation and littering. Fly tipping between sites 1 and 2 on the Taff Bargoed has also been observed. No wastewater treatment plants, or combined sewage overflows are known in the study area. The surrounding unmanaged heathland is used for sheep grazing without any known organic or artificial fertilisers being used on the land. The study area is characterised by steep hill slopes (30–40°), especially around the proximity of the mining area (Fig. 1C–D). The bed slope of the 2 km reach of the sampled Taff Bargoed is steep and relatively constant between sampling sites, with an average gradient of 1:3.43 (Fig. S1).

The Taff Bargoed flows for a total length of 11 km before entering the River Taff, which flows through the centre of Cardiff, Wales (UK). The source of the Taff Bargoed is located in the Ffos-y-fran mine (Merthyr Tydfil, Wales, UK) and flows around the perimeter of the mining spoils (Fig. 1A). The Taff Bargoed also drains the south and west sides of the mine's surface water. No access to the mining area was granted, so sampling was conducted on the Taff Bargoed as close as possible to the mine. The Ffos-y-fran mine is the UK's largest opencast coal mine, spanning more than 8 km<sup>2</sup> in area, with depths of up to 180 m. Between its opening in 2008 and 2023, the mine has produced more than 11 million tonnes of coal and has been responsible for 86% of the UK's total coal output in 2023 (National Statistics, 2022). The mine stopped actively mining for coal in November 2023 but continued to export coal from the mine with operations up until at least May 2024 (Coal Action Network, 2024). A land reclamation project with the aim of returning the area to its former use as common land for livestock grazing was pronounced in 2015 and planned to start in 2024 (Miller Argent & RPS, 2015).

The Taff Bargoed receives additional inflow from the Nant Gyrawd, which is a tributary draining the eastern side of the Ffos-y-fran mine. The confluence of the Nant Gyrawd with the Taff Bargoed is situated between MP sampling sites 4 and 5 (Fig. 1A) and the contributing catchment areas between sites 4 and 5 more than double due to the Nant Gyrawd tributary (Fig. 1E). As no access to the Nant Gyrawd was granted, sampling was conducted as close as possible to the confluence of the river at site 5. No access further downstream of site 5 was also

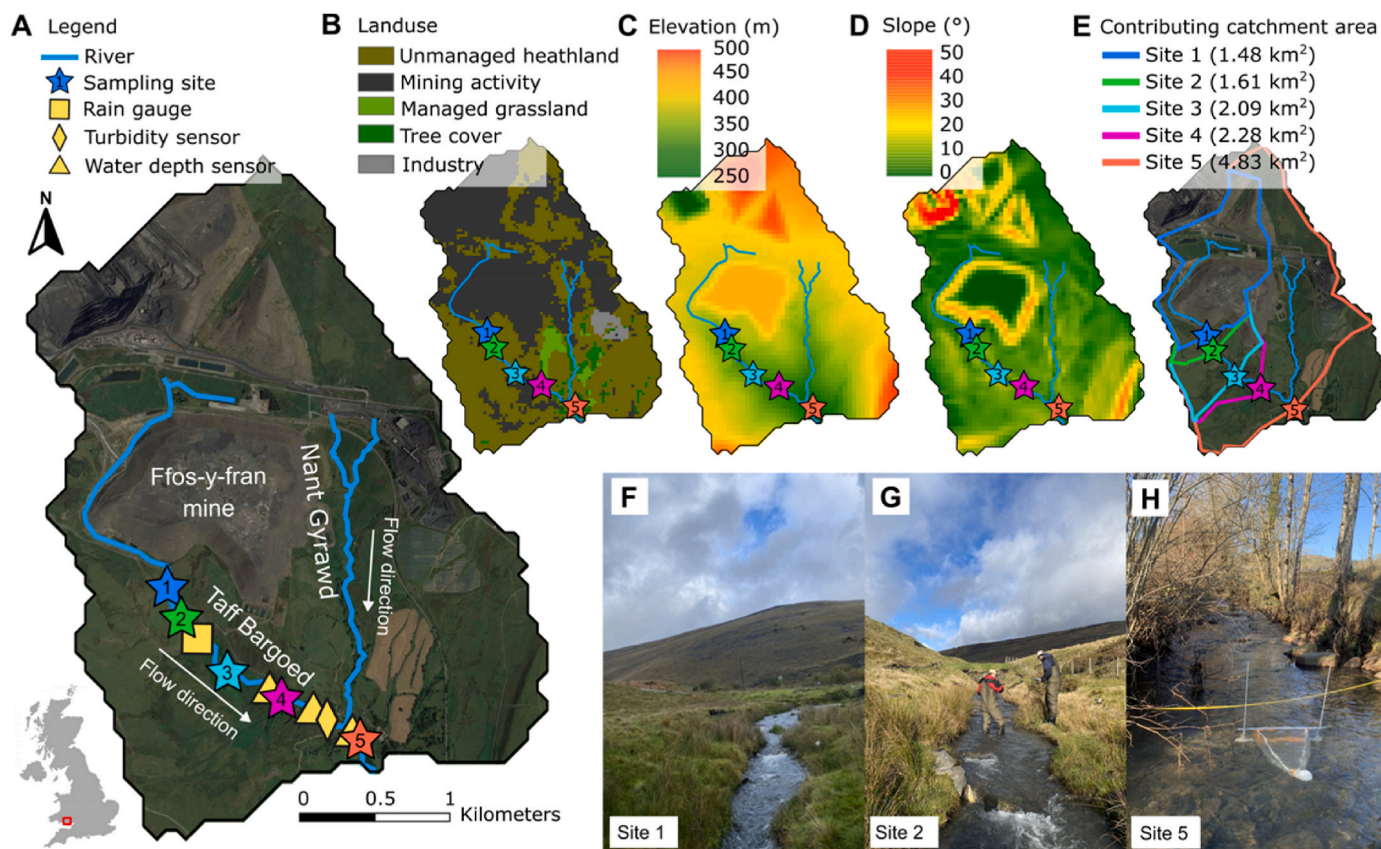


**Fig. 1.** A) The study area of the Taff Bargoed, showing the location of sampling sites, rain gauge, turbidity and water depth sensors. B-E) The study area characterisation undertaken on ArcGIS, showing the land use, elevation (5 m resolution Lidar DTM (Digimaps, 2024)), slope, and contributing catchment area for each sampling site. F-G) Photographs of sampling sites 1, 2 and 5 on the Taff Bargoed and the net used for sampling MPs.

granted. There are also a number of smaller ephemeral tributaries that are only present during high rainfall events that flow into the Taff Bargoed from the eastern and western hill slopes of the unmanaged heathland.

The riverbed grain size distribution of each sampling site on the Taff Bargoed was characterised by using sieve grain size analysis for the finer fraction of sediments ( $d < 10$  mm) (ISO, 2020) and a photogrammetry method for the top layer of larger gravel and cobble grain sizes ( $d > 10$  mm) using BASEGRAIN (Detert and Weitbrecht, 2013) (described in the Supplementary Materials S1). Granulometry curves that combine both techniques for each site are shown in Fig. S1. The  $d_{50}$  for all sites was calculated as between 5.74 and 10.81 mm, with a geometric standard deviation of the grain size ( $\sigma = \sqrt{d_{64}/d_{16}}$ ) between 2.25 and 5.62, which corresponds to a gravel bed river (Table S1).

## 2.2. Collection of MP samples and river flow characterisation

Five MP sampling sites on the Taff Bargoed were chosen for instream MP sampling. The five sites were approximately 500 m apart and chosen at straight sections of rivers to ensure flow through the net was relatively straight, with a flat riverbed (no bedforms or large boulders), constant slope and uniform channel width (Table S1). Sampling campaigns were conducted over a two-year period between January 2023 and April 2024. This was chosen to cover a least two seasonal variations of both summer and winter river flows and rainfall in the study area. Sampling campaigns between January 2023 to August 2023 only considered site 5 for MP sampling ( $N = 8$  campaigns), while sampling campaigns between November 2023–April 2024 considered all sites (sites 1–5) ( $N = 3$  campaigns). Sampling campaigns were conducted during dry weather conditions, between 4 and 282 h after rainfall events, to optimise the

chances of steady-state environmental conditions. This approach aimed to minimise potential temporal variability in the contributions of land-based MP to the river during the sampling period.

The river flow was characterised at each sampling site for every sampling campaign in terms of discharge ( $Q$ ), bulk velocity ( $V$ ) and thalweg flow depth ( $H$ ), which are presented in Table S2. River discharge was calculated using the velocity area method and a handheld electromagnetic flow meter (OTT MF Pro flow meter 0.001 resolution,  $\pm 0.015$  m/s accuracy) was used to measure the velocity. Further details regarding the measurements of flow velocities are presented in the Supplementary Materials S2

MPs were collected using a rectangular 0.25 m high, 0.4 m wide net, with mesh pore size of 250  $\mu\text{m}$  (Fig. 1H). The net had a cod end that consisted of a 300 mL bottle to collect the MPs. For every sampling site in every sampling campaign, three repeat samples were taken. For sampling, the net was placed at the riverbed at the thalweg of the river, meaning that the net collected MPs that were transported as bed load and suspended load. The net was deployed for a duration of time that would allow for more than 500 L of water to be passed through it, based on recommendations by (Koelmans et al., 2019; Lofty et al., 2023), which corresponded to 5–10 min per repeat sample. After each repeat sample, the net was rinsed using the river water to flush the MPs from the net's mesh into the cod end.

The volume of water sampled by the net was calculated as the calculated water discharge passing through the net, multiplied by the sampling duration. River depth varied between sampling campaigns and for some campaigns the top of the net was above the water surface, meaning the net's cross-sectional area was not fully covered by the water, which was taken into consideration in the calculations of the water volume. Due to the nets filtering efficiency, the flow velocity

inside the net may have been slightly lower than estimations made based on the average velocity of water flowing through the net's cross-sectional position in the river (Fraser, 1968; Smith et al., 1968). This means that estimated water volume filtered by the net may be greater than the actual volume, thus leading to a potential overestimation of the water volume and an underestimation of calculated MP concentration.

### 2.3. Instrumentation and data collection for catchment characterisation

To characterise the pre-existing conditions in the catchment area prior to MP sampling, a rainfall gauge, three water level sensors and a turbidity sensor were placed into the Taff Bargoed study site (see Fig. 1A for locations of instrumentation). A full description of the instrumentation is provided in Supplementary Materials S3.

### 2.4. Extraction and identification of microplastics and total suspended solids

After each sampling campaign, water samples were taken back to the lab and stored in cool dark conditions. MPs were isolated, identified and quantified from the water samples in six steps: (1) filtration, (2) quantification of total suspended solids (TSS) content, (3) wet peroxide oxidation using Fentons reagent, (4) density separation using zinc chloride (ZnCl<sub>2</sub>) (when required), (5) microscope identification and

quantification, and (6) Raman spectroscopy. A full description of each step used to isolate, identify and quantify the MPs from the samples is provided in the Supplementary Materials S4.

### 2.5. Polymer characterisation

Microplastic polymer type was identified using a Thermo Scientific DXR Raman microscope equipped with a 780 nm laser and 10 × objective. 20 mW of power at the sample using a 5second exposure and 3 accumulations was used to generate a single spectrum. The spectral peaks of 236 suspected MPs were analysed from site 5, which related to 28% of suspected MPs from site 5, which is equal to 15% of all MPs from all sites. 67% of the MPs were confirmed as plastic polymers by Raman spectroscopy. A full description of the Raman microscope protocol and spectral matching is described in the Supplementary Materials S5.

### 2.6. Spike tests and controls

To ensure that the extraction methodology for MPs was efficient from the river water samples, a spiked sample of 0.5 mm spheres was tested in unison of the river water samples. The spiked sample went through an analogous isolation procedure as the river samples, achieving recovery rates of 90%. A full description of the spike tests and control measures to minimise contamination of the samples and are also

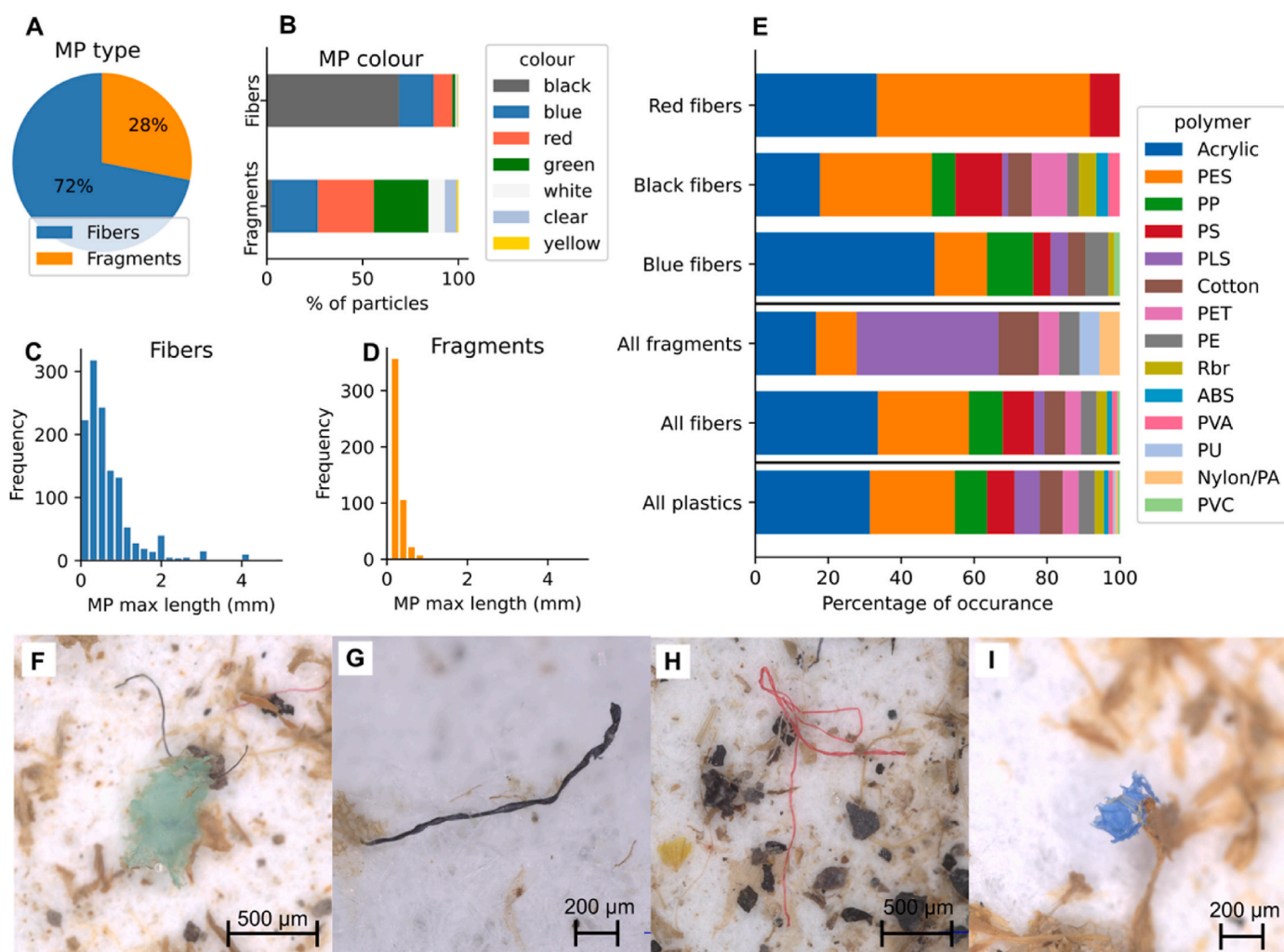


Fig. 2. Identified MPs in terms of A) MP type, B) MP colour, C) fiber maximum size distribution and D) fragment maximum size distribution. E) MP polymer types identified in the Taff Bargoed at site 5 by Raman spectroscopy. F) Photographs of a green fragment and black fiber, G) a black fiber, H) a red fiber, and I) a blue fragment found from MP samples. (For interpretation of the references to colour in this figure legend, the reader is referred to the Web version of this article.)

described in the Supplementary Materials S6.

### 3. Results and discussion

#### 3.1. MP characteristics

A total of 1,801 MP particles were identified from all sampling sites and sampling campaigns on the Taff Bargoed. Fig. 2A–D presents the characteristics of the MPs identified from the Taff Bargoed samples, Fig. 2E presents the polymer types of MPs identified at site 5 using Raman spectroscopy, and Fig. 2F–I shows photographs of some of the identified MPs. Results showed that 72% of the identified MPs were fibers, while 28% were fragments (Fig. 2A). For fibers, the most common colours were black (68%), blue (10%) and red (6%), while for fragments the most frequent colours were green (25%), red (24%) and blue (23%) (Fig. 2B). On average, fibers had a longer maximum length compared to fragments, with an average length of 0.77 mm for fibers and 0.28 mm for fragments (Fig. 2C and D).

The most common polymer types identified in the Taff Bargoed at site 5 were acrylic (31%), polyester (PES) (23%), polypropylene (PP) (9%), polystyrene (PS) (8%), and polysulfone (PLS) (7%) (Fig. 2E). Fibers identified in the Taff Bargoed were mostly composed of either acrylic (33%) or PES (25%). Blue fibers were mostly composed of acrylic polymers (49%), while black (30%) and red fibers (58%) were largely PES.

The precise origin of the fibers in the samples is challenging to determine due to the variety of potential sources in the study area. Fibers may have originated from the shedding of underground geotextiles used for soil stabilization, drainage, or erosion control that are used in and around mining sites and which commonly use acrylic and PES polymers in their construction (European Environmental Agency, 2024). The fibers may also have originated from the degradation of equipment, such as dump bags observed to be used to transport waste material from the mine, or from the shedding of clothing worn by mine workers (Cole

et al., 2011). Fragments identified from samples were mostly composed of PLS (39%), a thermoplastic designed for its strength and stability at high temperatures and resistance to chemicals. PLS is a commonly used polymer for hardwearing plastic equipment or for membranes in wastewater treatment, which may have been used in the wastewater treatment systems of the Ffos-y-fran coal mine water discharge (Mamah et al., 2021; Yu et al., 2024).

#### 3.2. MP variation, rainfall and river flow

Daily rainfall, water depth and turbidity readings over the entire sampling period (January 2023–April 2024) from the installed loggers are shown in Fig. 3A, while the river discharge measured at site 5 on the Taff Bargoed, downstream of the Nant Gyrawd confluence, for each sampling campaign is shown in Fig. 3B. Discharge in the Taff Bargoed at site 5 on sampling dates ranges from baseflow conditions 0.06 m<sup>3</sup>/s to high flow 0.52 m<sup>3</sup>/s (Fig. 3B). The average MP concentration and MP load at site 5 are plotted in Fig. 3C and D, respectively, with different colours representing different MP sampling campaigns. The full data set is available in Table S3. At site 5, instream MP concentrations range between 1.34 and 28.87 MP/m<sup>3</sup>, with an average of 14.6 ± 10.31 MP/m<sup>3</sup>, while MP load ranged over an order of magnitude from 0.44 to 3.04 MP/s with an average of 1.42 ± 0.81 MP/s (Fig. 3C and D).

These MP concentrations and loads should be seen as conservative estimates due to the methodology used to measure water volume filtered by the sampling net (Fraser, 1968; Smith et al., 1968) (see Section 2.2 Collection of MP samples and river flow characterisation). The cessation of active mining at Ffos-y-Fran in November 2023 appears to have had no impact on the number of MPs observed in the Taff Bargoed (Fig. 3).

To correlate the variation of instream MPs to hydrological and hydraulic factors in the catchment, MP concentration and MP load is plotted against the number of dry weather hours prior to a sampling campaign in Fig. 4A and B, and river discharge in Fig. 4C and D, respectively. MP concentrations are strongly positively exponential

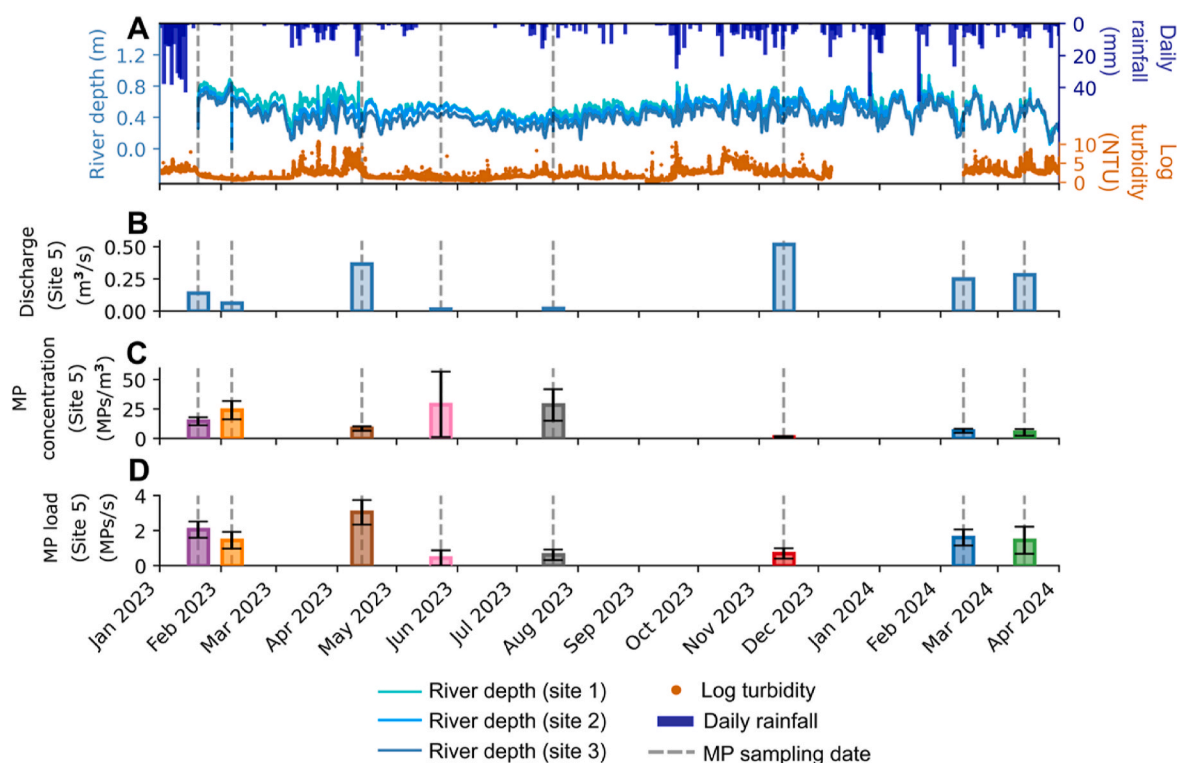
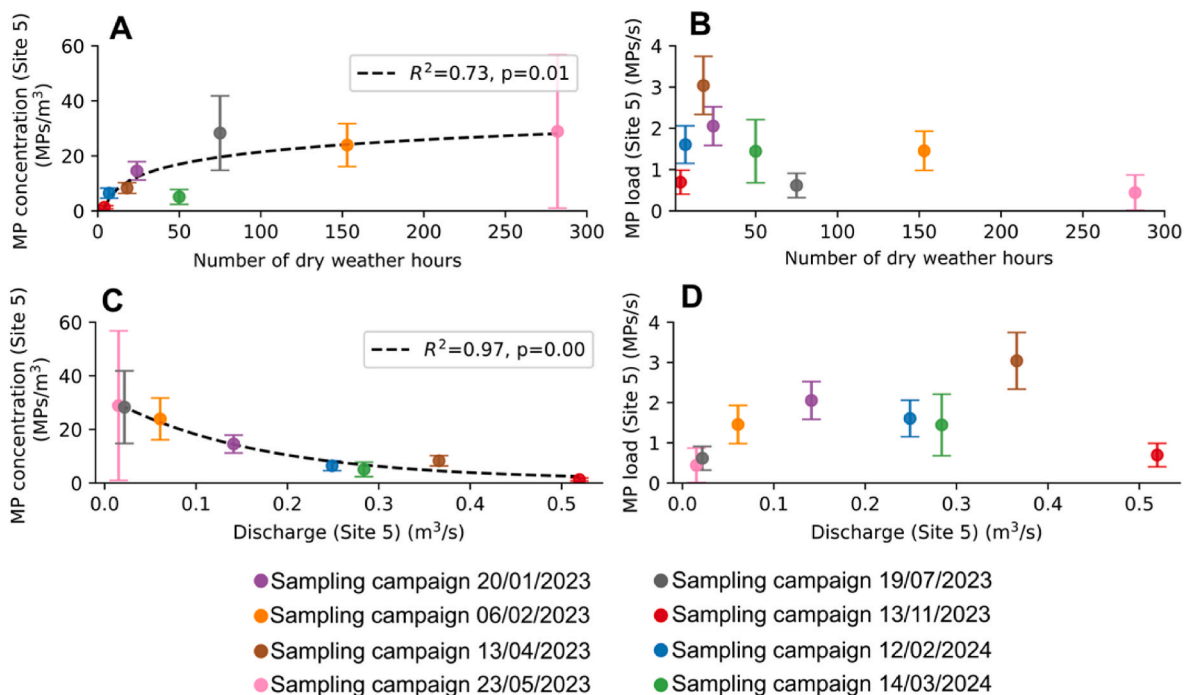


Fig. 3. A) Times series of rainfall, river depth and turbidity readings from the Taff Bargoed. No turbidity data is available for the period between January–March 2024. B–D) The measured river discharge, average MP concentration and MP load at site 5 for every MP sampling campaign, with error bars displaying the standard deviation of the result.



**Fig. 4.** A-B) The average MP concentration and MP load for each sampling campaign plotted against the number of dry hours prior to a sampling campaign and C-D) river discharge at site 5. The different coloured markers denote the different MP sampling campaign dates. Dashed lines represent an exponential regression with calculated  $R^2$  values and Spearman rank test  $p$  values.

relationship) correlated with the number of dry weather hours (Fig. 4A) ( $R^2 = 0.73$ , Spearman rank test  $p < 0.01$ ) and a strongly negatively (exponential relationship) correlated to river discharge (Fig. 4C) ( $R^2 = 0.97$ , Spearman rank test  $p < 0.001$ ). On the other hand, a negligible relationship between MP load, number of dry weather hours and river discharge was observed in the Taff Bargoed (Fig. 4B and D), which suggests MP load does not respond to variations in MP concentration,

discharge and rainfall in the Taff Bargoed catchment.

The results indicate a dilution effect on the instream MP concentration, whereby rainfall events occurring close to a sampling campaign resulted in higher river discharges and lower MP concentrations (Fig. 4A and C). This is an indication of source limitation, due to low stocks of land-based MPs available to be mobilised for transport into the river during rainfall events, as well as the runoff volume diluting the already-

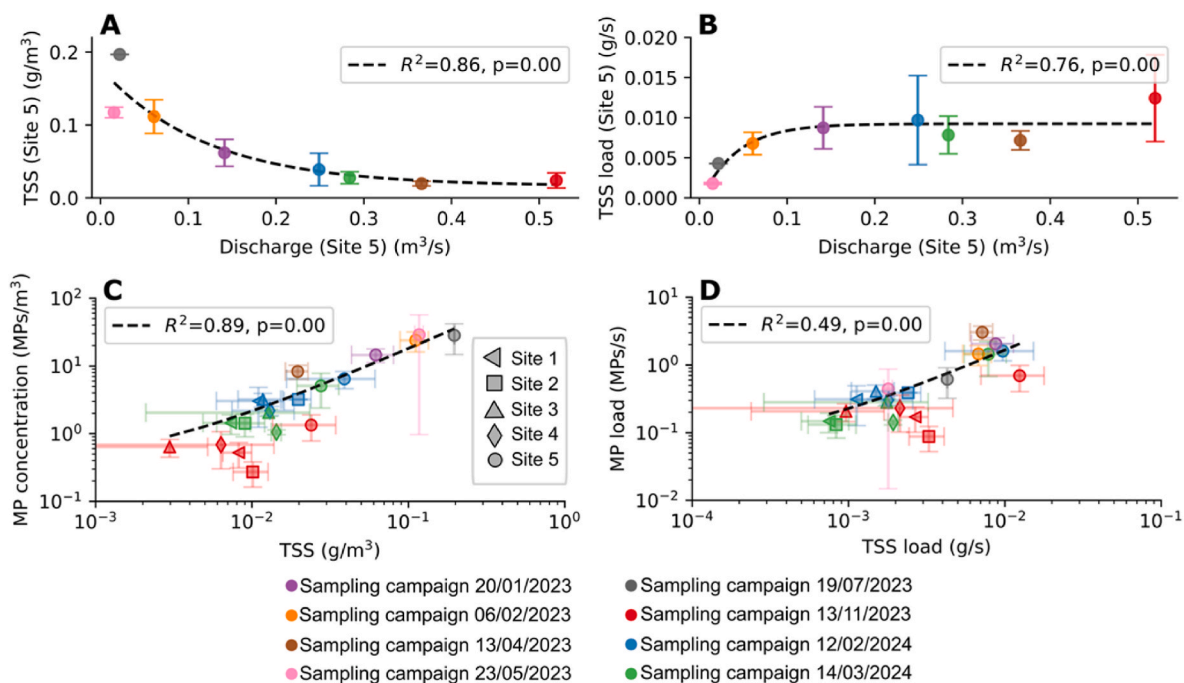


**Fig. 5.** A) Total suspended solids (TSS) and B) TSS load plotted against river discharge for site 5. C) MP concentration plotted against TSS at sampling sites 1–5 on the Taff Bargoed in log-log scale, D) MP load plotted against TSS load in log-log scale. Error bars represent the standard deviation of the result. The different coloured markers represent the MP sampling campaign dates. Dashed lines represent a linear regression with calculated  $R^2$  values and Spearman rank test  $p$  values.

present MPs concentration in the river. Although this is a singular example from one rural catchment, the result suggests that concentrations of MPs in the Taff Bargoed decrease due to the increase in rainfall volume, contrasting with previous studies conducted in more urban environments, which suggest MP concentration increases with rainfall (Schmidt et al., 2018; Wagner et al., 2019; Hitchcock, 2020; Moses et al., 2023). On the other hand, in periods of dry weather, where no rainfall had occurred for approximately 72 h, and the river is returning to baseflow conditions, MP concentration was higher and had a relatively constant relationship with discharge, as no dilution effect is observed (Fig. 4A). The MP contribution to the Taff Bargoed during periods of no rainfall is likely from the mine's groundwater and/or atmospheric deposition, although the exact source cannot be definitively proven without further investigation.

### 3.3. MPs and total suspended solids

Fig. 5A presents the relationship between TSS and river discharge for site 5, while Fig. 5B shows the relationship between TSS load and river discharge. Results indicated that TSS is negatively correlated with discharge at site 5 ( $R^2 = 0.86$ , Spearman rank test  $p < 0.001$ ) (Fig. 5A), which is the analogous to the relationship observed with MP concentration (as seen in Fig. 4C), suggesting that a similar dilution effect is observed for suspended solids in the Taff Bargoed. This indicates that similar transport mechanisms affect MPs and other suspended solids running off the land in the Taff Bargoed catchment in response to rainfall events. On the other hand, there is a relatively positive relationship

between TSS load and discharge at low river discharges, which becomes relatively constant once the river discharge reaches approximately  $0.15 \text{ m}^3/\text{s}$ . This differs from the negligible relationship observed between MP load and discharge (as seen in Fig. 4D).

Fig. 5C presents the relationship between MP concentration and TSS for all sites, while Fig. 5D shows the relationship between MP load and TSS load. MP concentration and TSS are strongly correlated by a linear relationship ( $R^2 = 0.89$ , Spearman rank test  $p < 0.001$ ) due to their similarities in their responses to river discharge. This suggests that TSS may represent a useful proxy for estimating MP variation in the Taff Bargoed. On the other hand, a reduced linear relationship between MP load and TSS load is observed ( $R^2 = 0.49$ , Spearman rank test  $p < 0.001$ ) (Fig. 5D), due to their differences in their relationships with river discharge.

### 3.4. Reach-scale longitudinal variation

Longitudinal variation of MP abundance in the Taff Bargoed was assessed by the MP concentration and MP load for increasing distance downstream (Sites 1–5) (Fig. 1A) for three sampling campaigns (November 2023–April 2024). Fig. 6A–C shows the MP concentration at each sampling site against the longitudinal downstream distance (zero datum is the Taff Bargoed source located in the Ffos-y-fran mine), discharge and drainage area, respectively, while Fig. 6D–F and G–H shows the same for MP load and TSS, respectively.

Results show that MPs concentration, MP load and TSS remain

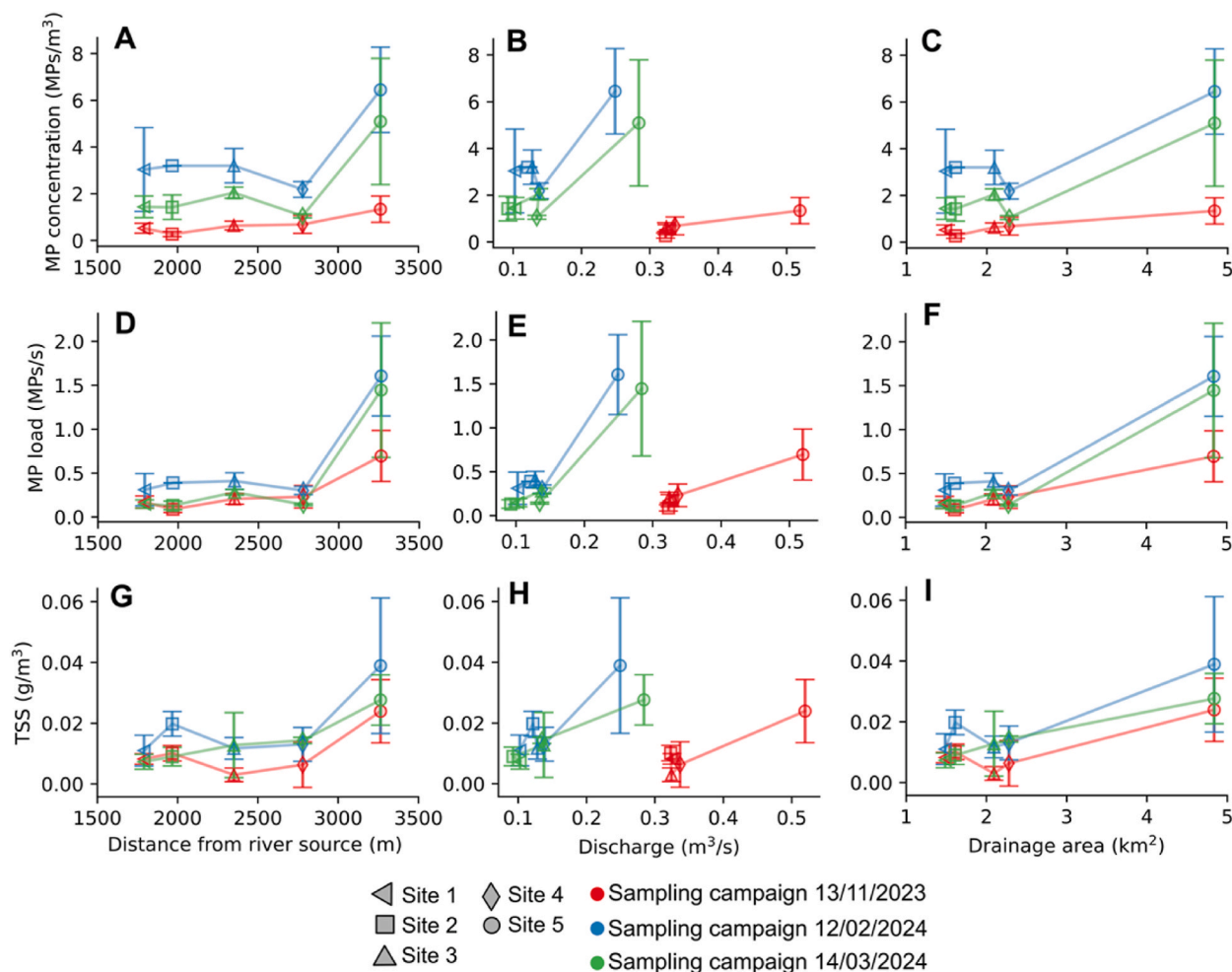


Fig. 6. MP concentration, MP load and total suspended solids (TSS) at sampling sites 1–5 on the Taff Bargoed for three sampling campaigns, plotted against the longitudinal distance from river source (zero datum is the Taff Bargoed source), river discharge and drainage area.

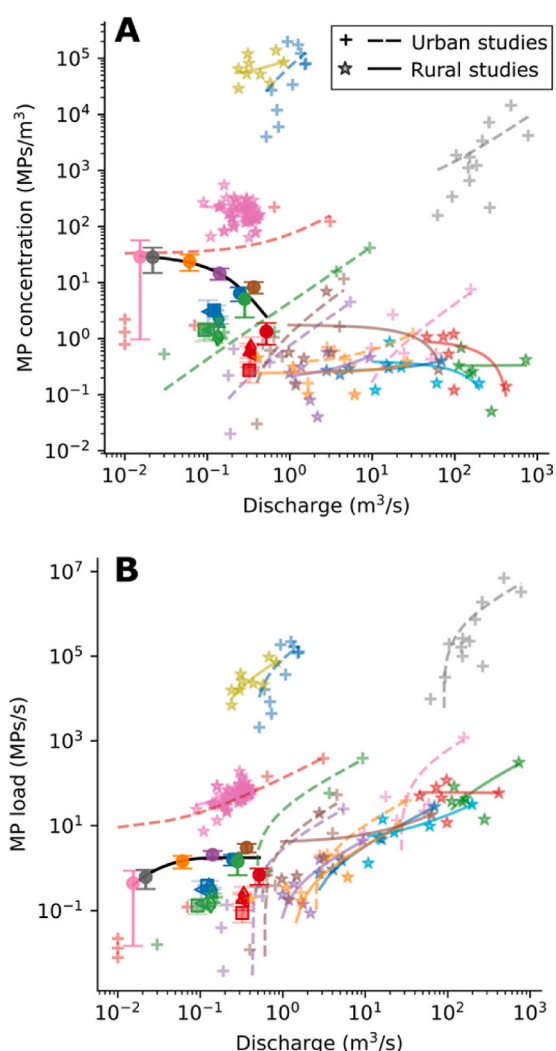
relatively constant between sites 1 and 4, where discharge and drainage area are similar, and where there are no significant inflows into the Taff Bargoed (Fig. 6). This indicates that the surrounding rural land between sites 1–4 are not contributing to the instream concentration of MPs. It is observed that river discharge, MP concentration, MP load and TSS all significantly increase at site 5 for all sampling dates, due to the inflow of the Nant Gyrawd between sites 4 and 5 (Fig. 6). Data indicate that the Nant Gyrawd increases MP concentration at site 5 by a factor of 2–4 and MP load by a factor of 5–10. This suggests that the Nant Gyrawd, which drains the eastern side of the Ffos-y-fran mine (Fig. 1A), contributes a significant amount of MPs and suspended solids to the Taff Bargoed.

Since site 1 is less than 2 km from the source of the Taff Bargoed, which is located in the Ffos-y-fran coal mine and drains the southern and western sides of the mine (Fig. 1A), it suggests that a significant portion of the MPs in the Taff Bargoed, and subsequently transported downstream, may originate from the mine’s overland or groundwater drainage. Although it cannot be definitively proven that the Ffos-y-fran coal mine is the main source of MPs in the Taff Bargoed, evidence suggests it is a significant contributor. While MPs could also be introduced to the river through wind-driven atmospheric deposition (Zhang et al., 2019) or from the breakdown of plastics due to fly-tipping observed between sites 1 and 2, the lack of an increase in MP concentration

between sites 1 and 4, combined with the limited alternative sources of MPs in this remote catchment, points to the Ffos-y-fran coal mine as a likely contributor of MPs to the Taff Bargoed.

### 3.5. Intercomparison between rural and urban studies

To compare the instream MP concentration and MP load for the rural catchment of the Taff Bargoed, with other MP studies conducted in both rural and urban catchments, Fig. 7 shows MP concentration (Fig. 7A) and MP load (Fig. 7B) plotted against river discharge for all sites at the Taff Bargoed, with data from urban and rural reaches of the Parthe River (Germany) (Wagner et al., 2019), urban and rural reaches of the Neuse River basin (USA) (Kurki-Fox et al., 2023), urban reaches of the Weser river (Germany) (Moses et al., 2023) and rural reaches of Eastcote Brook (UK) (Kukkola et al., 2024). All comparative data shown in Fig. 7 are from the same sampling locations on the selected rivers, over different river discharges, similar to the study methodology presented herein. The Neuse River and Weser River are comparatively much larger rivers (river catchments 10,000–49,000 km<sup>2</sup>) to the Taff Bargoed and Eastcote Brook (1–5 km<sup>2</sup>) and the rural reaches of the Neuse River basin were classified as catchments with less than 50% urban development (Kurki-Fox et al., 2023). Full details of the compared studies and their



#### This study

- Sampling campaign 20/01/2023 (This study)
- Sampling campaign 06/02/2023 (This study)
- Sampling campaign 13/04/2023 (This study)
- Sampling campaign 23/05/2023 (This study)
- Sampling campaign 19/07/2023 (This study)
- Sampling campaign 13/11/2023 (This study)
- Sampling campaign 12/02/2024 (This study)
- Sampling campaign 14/03/2024 (This study)

#### Other rural catchments

- ★ Parthe River (Germany) (Wagner et al. 2019)
- ★ Contentnea Creek (USA) (Kurki-Fox et al. 2023)
- ★ Little River Princeton (USA) (Kurki-Fox et al. 2023)
- ★ Little River Zebulon (USA) (Kurki-Fox et al. 2023)
- ★ Neuse River Fort Barnwell (USA) (Kurki-Fox et al. 2023)
- ★ Neuse River Goldsboro (USA) (Kurki-Fox et al. 2023)
- ★ Swift Creek Clayton (USA) (Kurki-Fox et al. 2023)
- ★ Trent River (USA) (Kurki-Fox et al. 2023)
- ★ Eastcote Brook (UK) (Kukkola et al. 2024)

#### Other urban catchments

- ✦ Parthe River (Germany) (Wagner et al. 2019)
- ✦ Crabtree Creek (USA) (Kurki-Fox et al. 2023)
- ✦ Marsh Creek (USA) (Kurki-Fox et al. 2023)
- ✦ Rocky Branch (USA) (Kurki-Fox et al. 2023)
- ✦ Swift Creek Apex (USA) (Kurki-Fox et al. 2023)
- ✦ Walnut Creek (USA) (Kurki-Fox et al. 2023)
- ✦ Neuse River Clayton (USA) (Kurki-Fox et al. 2023)
- ✦ River Weser (Germany) (Moses et al. 2023)

Fig. 7. A) MP concentration and B) MP load in the Taff Bargoed against river discharge for all sites in log-log scale, plotted with MP data from urban and rural reaches of the Parthe River (Germany) (Wagner et al., 2019), urban and rural reaches of the Neuse River (USA) (Kurki-Fox et al., 2023), urban reaches of the Weser River (Germany) (Moses et al., 2023) and rural reaches of Eastcote Brook (UK) (Kukkola et al., 2024). Rural studies are shown with star markers, with a linear regression in a solid line, while urban studies are shown with cross markers, with a linear regression in a dashed line. Regression for the Taff Bargoed is shown in a solid black line and only includes an exponential regression line for site 5, analogous to Fig. 4.

context are available in the supplementary material (Table S4).

MP concentration and MP load are significantly lower in the Taff Bargoed compared to the Parthe River and Weser River, likely due to higher number of MP sources in the these larger catchments (Table S4), but are relatively similar to urban and rural reaches of the Neuse River basin (Fig. 7). On the whole, the relationship between MP concentration and river discharge in the Taff Bargoed is consistent with other studies conducted in rural catchments, which typically show a negative or negligible relationship (Fig. 7A, star markers and solid regression lines) (Barrows et al., 2018; Wagner et al., 2019; Kurki-Fox et al., 2023; Kukkola et al., 2024). This correlation is largely attributed to source limitation processes, where MP sources are fewer and less abundant in a rural and remote environment, and therefore a limited stock of land-based MPs is available to be mobilised into the river with rainfall, which cannot keep up with the increase of stream flow, leading to a dilution effect on the MP concentration. This contrasts with studies conducted in more urban and populated rivers, which have generally found positive correlations between MP concentration and discharge (Fig. 7A, cross markers and dashed regression lines) (Wagner et al., 2019; Kurki-Fox et al., 2023; Moses et al., 2023). This is largely due to transport limited processes, where there are abundant sources of MP in an urban and populated catchment, which are active and proportionally supplying MPs to the river. This contrast between rural and urban rivers is critical for targeted management of MPs as it highlights the need for differentiated strategies between the two land usages.

For MP load, there is generally either no correlation or a positive correlation between MP load and river discharge, regardless of whether the study was conducted a rural or urban settling (Fig. 7B). This indicates that MP load is largely dependent on the volume of water transported in the river, rather than the initial concentration of MPs within the water and the surrounding land usage, which influence the source and transport limiting processes. Consequently, the number of MPs transported in river systems potentially increases with greater river discharges for the studies compared in Fig. 7.

#### 4. Conclusions

This study reports the results of a two-year investigation of the variation of instream MP concentration and MP load at five sites along a 2 km long reach of the Taff Bargoed River, sourced from the UK's largest opencast coal mine and situated in a remote upper catchment area in Wales, UK. Small fibers (<1 mm) composed of acrylic and polyester (PES) dominated the MP samples, while less commonly observed fragments were mostly composed of polysulfone (PLS). MP concentration in the Taff Bargoed was diluted by rainfall occurring prior to MP sampling campaigns and subsequent increase in river discharge and is governed by source limitation processes. This contrasts with results found in rivers located in urban and populated areas, where transport limited processes largely dictate MP concentration flux. The differing limiting processes that govern MP concentration in rural and urban rivers are key for managing MPs effectively, as it underscores the need for strategies tailored to watersheds with different land usages. MP concentration also had a strong positive relationship with total suspended solids, suggesting that total suspended solids may represent a useful proxy for estimating MP variation, aiding in future MP monitoring campaigns. Overall, data suggests that the Ffos-y-fran coal mining activity is likely a major contributor of MPs to the Taff Bargoed River given the proximity of the mine to the source of the river and the lack of other substantial sources of MPs in the rural catchment. These findings are important to provide evidence of the hydraulic and hydrological mechanisms that regulate MPs from diffuse sources of pollution in a mixed-use rural environment, which gives insights into how to manage and mitigate their release into aquatic systems.

#### CRedit authorship contribution statement

**James Lofty:** Writing – review & editing, Writing – original draft, Visualization, Methodology, Investigation, Formal analysis, Data curation, Conceptualization. **Guglielmo Sonnino Soriso:** Writing – review & editing, Methodology, Investigation, Data curation, Conceptualization. **Liam Kelleher:** Writing – review & editing, Methodology, Investigation. **Stefan Krause:** Writing – review & editing, Methodology, Investigation. **Pablo Ouro:** Writing – review & editing, Supervision, Methodology, Funding acquisition, Conceptualization. **Catherine Wilson:** Writing – review & editing, Supervision, Methodology, Investigation, Funding acquisition, Conceptualization.

#### Funding sources

UK Engineering and Physical Sciences Research Council (EPSRC) grant number EP/T517951/1 (JL).

Taff Bargoed Catchment Restoration Project (Merthyr Tydfil County Borough Council).

#### Declaration of competing interest

The authors declare that they have no known competing financial interests or personal relationships that could have appeared to influence the work reported in this paper.

#### Acknowledgements

The authors are grateful to Max Maywood and Darren De Xuen Loh for helping with field work and processing of microplastic samples. We are also grateful for Amanda Kitching for supervision of sediment analysis, as well as Rachel Morton and Gillian Hampson at Merthyr Tydfil County Borough Council for access to field sites and funding acquisition.

#### Appendix A. Supplementary data

Supplementary data to this article can be found online at <https://doi.org/10.1016/j.envpol.2025.125722>.

#### Data availability

data available at: <https://doi.org/10.5281/zenodo.14707892>.

#### References

- Amereh, F., et al., 2022. Placental plastics in young women from general population correlate with reduced foetal growth in IUGR pregnancies. *Environ. Pollut.* 314, 120174. Available at: <https://linkinghub.elsevier.com/retrieve/pii/S0269749122013884>.
- Baas, J.H., et al., 2022. Blood, lead and spheres: a hindered settling equation for sedimentologists based on metadata analysis. *The Depositional Record* 8 (2), 603–615. Available at: <https://onlinelibrary.wiley.com/doi/10.1002/dep2.176>.
- Barrows, A.P.W., Christiansen, K.S., Bode, E.T., Hoellein, T.J., 2018. A watershed-scale, citizen science approach to quantifying microplastic concentration in a mixed land-use river. *Water Res.* 147, 382–392. Available at: <https://linkinghub.elsevier.com/retrieve/pii/S0043135418308078>.
- Brožová, K., Halfar, J., Cabanová, K., Motyka, O., Drabinová, S., Hanus, P., Heviánková, S., 2023. The first evidence of microplastic occurrence in mine water: the largest black coal mining area in the Czech Republic. *Water Res.* 244, 120538. Available at: <https://linkinghub.elsevier.com/retrieve/pii/S0043135423009788>.
- Cho, Y., Shim, W.J., Ha, S.Y., Han, G.M., Jang, M., Hong, S.H., 2023. Microplastic emission characteristics of stormwater runoff in an urban area: intra-event variability and influencing factors. *Sci. Total Environ.* 866, 161318. Available at: <https://linkinghub.elsevier.com/retrieve/pii/S0048969722084224>.
- Coal Action Network, 2024. Ffos-y-fran: Timeline of Illegal Coal Mining.
- Cole, M., Lindeque, P., Halsband, C., Galloway, T.S., 2011. Microplastics as contaminants in the marine environment: a review. *Mar. Pollut. Bull.* 62 (12), 2588–2597. Available at: <http://www.sciencedirect.com/science/article/pii/S0025326X11005133>.
- Crossman, J., Hurley, R.R., Futter, M., Nizzetto, L., 2020. Transfer and transport of microplastics from biosolids to agricultural soils and the wider environment. *Sci.*

- Total Environ. 724, 138334. Available at: <http://www.sciencedirect.com/science/article/pii/S0048969720318477>.
- Detert, M., Weitbrecht, V., 2013. User guide to gravelometric image analysis by BASEGRAIN. Available at: [www.basement.ethz.ch/services/Tools/](http://www.basement.ethz.ch/services/Tools/).
- Dick Vethaak, A., Legler, J., 2021. Microplastics and human health. *Science* 371 (6530), 672–674. Available at: <https://www.science.org/doi/10.1126/science.abe5041>.
- Digimaps, 2024. Digimaps - society. Available at: <https://digimap.edina.ac.uk/roam/map/society>.
- European Environmental Agency, 2024. Microplastics Unintentionally Released into the Environment in the EU.
- Feng, S., Lu, H., Tian, P., Xue, Y., Lu, J., Tang, M., Feng, W., 2020. Analysis of microplastics in a remote region of the Tibetan Plateau: implications for natural environmental response to human activities. *Sci. Total Environ.* 739, 140087. <https://doi.org/10.1016/J.SCITOTENV.2020.140087>.
- Fraser, J.H., 1968. The history of plankton sampling. *Zooplankton Sampling: Review Papers of the Proceedings of the Symposium on the Hydrodynamics of Zooplankton Sampling*. UNESCO, pp. 11–18.
- González-Fernández, D., Roebroek, C.T.J., Laufkötter, C., Cózar, A., van Emmerik, T.H.M., 2023. Diverging estimates of river plastic input to the ocean. *Nat. Rev. Earth Environ.* 4 (7), 424–426, 4(7). <https://www.nature.com/articles/s43017-023-00448-3>.
- Grbić, J., Helm, P., Athey, S., Rochman, C.M., 2020. Microplastics entering northwestern Lake Ontario are diverse and linked to urban sources. *Water Res.* 174, 115623. <https://doi.org/10.1016/J.WATRES.2020.115623>.
- Han, N., Zhao, Q., Ao, H., Hu, H., Wu, C., 2022. Horizontal transport of macro- and microplastics on soil surface by rainfall induced surface runoff as affected by vegetations. *Sci. Total Environ.* 831, 154989. <https://doi.org/10.1016/j.scitotenv.2022.154989>.
- Hitchcock, J.N., 2020. Storm events as key moments of microplastic contamination in aquatic ecosystems. *Sci. Total Environ.* 734, 139436. Available at: <https://www.sciencedirect.com/science/article/pii/S0048969720329533>.
- Huang, Y., Liu, Q., Jia, W., Yan, C., Wang, J., 2020. Agricultural plastic mulching as a source of microplastics in the terrestrial environment. *Environ. Pollut.* 260, 114096. Available at: <http://www.sciencedirect.com/science/article/pii/S0269749119362475>.
- ISO, 2020. Soil Quality-Determination of Particle Size Distribution in Mineral Soil Material-Method by Sieving and Sedimentation. ISO 11277:2020.
- Jenner, L.C., Rotchell, J.M., Bennett, R.T., Cowen, M., Tentzeris, V., Sadofsky, L.R., 2022. Detection of microplastics in human lung tissue using  $\mu$ FTIR spectroscopy. *Sci. Total Environ.* 831, 154907. <https://doi.org/10.1016/J.SCITOTENV.2022.154907>.
- Koelmans, A.A., Mohamed Nor, N.H., Hermens, E., Kooi, M., Mintenig, S.M., De France, J., 2019. Microplastics in freshwaters and drinking water: critical review and assessment of data quality. *Water Res.* 155, 410–422. Available at: <http://www.sciencedirect.com/science/article/pii/S0043135419301794>.
- Krause, S., et al., 2021. Gathering at the top? Environmental controls of microplastic uptake and biomagnification in freshwater food webs. *Environ. Pollut.* 268, 115750. <https://doi.org/10.1016/J.ENVPOL.2020.115750>.
- Krause, S., et al., 2024. The potential of micro- and nanoplastics to exacerbate the health impacts and global burden of non-communicable diseases. *Cell Reports Medicine*, 101581. <https://doi.org/10.1016/j.xcrm.2024.101581>.
- Kukkola, A., et al., 2023. Prevailing impacts of river management on microplastic transport in contrasting US streams: rethinking global microplastic flux estimations. *Water Res.* 240, 120112. <https://doi.org/10.1016/J.WATRES.2023.120112>.
- Kukkola, A., et al., 2024. Snapshot sampling may not be enough to obtain robust estimates for riverine microplastic loads. *ACS ES and T Water* 4 (5), 2309–2319. Available at: <https://pubs.acs.org/doi/full/10.1021/acsestwater.4c00176>.
- Kunz, A., Schneider, F., Anthony, N., Lin, H.T., 2023. Microplastics in rivers along an urban-rural gradient in an urban agglomeration: correlation with land use, potential sources and pathways. *Environ. Pollut.* 321, 121096. <https://doi.org/10.1016/J.ENVPOL.2023.121096>.
- Kurki-Fox, J.J., et al., 2023. Microplastic distribution and characteristics across a large river basin: insights from the Neuse River in North Carolina, USA. *Sci. Total Environ.* 878, 162940. <https://doi.org/10.1016/J.SCITOTENV.2023.162940>.
- Leslie, H.A., van Velzen, M.J.M., Brandsma, S.H., Vethaak, A.D., Garcia-Vallejo, J.J., Lamoree, M.H., 2022. Discovery and quantification of plastic particle pollution in human blood. *Environ. Int.* 163, 107199. <https://doi.org/10.1016/J.ENVINT.2022.107199>.
- Lofty, J., Muhawenimana, V., Wilson, C.A.M.E., Ouro, P., 2022. Microplastics removal from a primary settler tank in a wastewater treatment plant and estimations of contamination onto European agricultural land via sewage sludge recycling. *Environ. Pollut.* 304, 119198. Available at: <https://linkinghub.elsevier.com/retrieve/pii/S0269749122004122>.
- Lofty, J., Ouro, P., Wilson, C.A.M.E., 2023. Microplastics in the riverine environment: meta-analysis and quality criteria for developing robust field sampling procedures. *Sci. Total Environ.* 863, 160893. Available at: <https://linkinghub.elsevier.com/retrieve/pii/S0048969722079967>.
- MacLeod, M., Arp, H.P.H., Tekman, M.B., Jahnke, A., 2021. The global threat from plastic pollution. *Science* 373 (6550), 61–65. Available at: <https://www.science.org/doi/10.1126/science.aba5433>.
- Mai, L., Sun, X.F., Xia, L.L., Bao, L.J., Liu, L.Y., Zeng, E.Y., 2020. Global riverine plastic outflows. *Environ. Sci. Technol.* 54 (16), 10049–10056. Available at: <https://pubs.acs.org/doi/abs/10.1021/acs.est.0c02273>.
- Mamah, S.C., Goh, P.S., Ismail, A.F., Suzaimi, N.D., Yogarathinam, L.T., Raji, Y.O., El-badawy, T.H., 2021. Recent development in modification of polysulfone membrane for water treatment application. *J. Water Proc. Eng.* 40, 101835. <https://doi.org/10.1016/J.JWPE.2020.101835>.
- Mani, T., Hauk, A., Walter, U., Burkhardt-Holm, P., 2015. Microplastics profile along the rhine river. *Sci. Rep.* 5 (1), 17988. Available at: <http://www.nature.com/articles/srep17988/>.
- Miller Argent & RPS, 2015. FFOS-Y-FRAN LAND RECLAMATION SCHEME RESTORATION PLAN. Available at: <https://www.merthyr.gov.uk/media/5004/ed039-ffos-y-fran-land-reclamation-scheme-restoration-plan-discharge-of-condition-5-3-delegated-report.pdf>.
- Moses, S.R., Löder, M.G.J., Herrmann, F., Laforsch, C., 2023. Seasonal variations of microplastic pollution in the German River Weser. *Sci. Total Environ.* 902, 166463. Available at: <https://linkinghub.elsevier.com/retrieve/pii/S004896972305088X>.
- National Statistics, 2022. Digest of UK Energy Statistics (DUKES): Solid Fuels and Derived Gases - GOV. UK. Available at: <https://www.gov.uk/government/statistics/solid-fuels-and-derived-gases-chapter-2-digest-of-united-kingdom-energy-statistics-duk>.
- Nava, V., et al., 2023. Plastic debris in lakes and reservoirs. *Nature* 619 (7969), 317–322, 619(7969). <https://www.nature.com/articles/s41586-023-06168-4>.
- Nizzetto, L., Futter, M., Langaas, S., 2016. Are agricultural soils dumps for microplastics of urban origin? *Environ. Sci. Technol.* 50 (20), 10777–10779. <https://doi.org/10.1021/acs.est.6b04140>.
- Persson, L., et al., 2022. Outside the safe operating space of the planetary boundary for novel entities. *Environ. Sci. Technol.* 56 (3), 1510–1521. <https://pubs.acs.org/doi/full/10.1021/acs.est.1c04158>.
- Pinlova, B., Nowack, B., 2024. From cracks to secondary microplastics - surface characterization of polyethylene terephthalate (PET) during weathering. *Chemosphere* 352. <https://doi.org/10.1016/j.chemosphere.2024.141305>.
- Qi, Y., et al., 2018. Macro- and micro- plastics in soil-plant system: effects of plastic mulch film residues on wheat (*Triticum aestivum*) growth. *Sci. Total Environ.* 645, 1048–1056. Available at: <https://www.sciencedirect.com/science/article/pii/S0048969718327219>.
- Ragusa, A., et al., 2022. Deeply in plasticenta: presence of microplastics in the intracellular compartment of human placentas. *Int. J. Environ. Res. Publ. Health* 19 (18). Available at: <https://pubmed.ncbi.nlm.nih.gov/36141864/>.
- Schmidt, L.K., Bochow, M., Imhof, H.K., Oswald, S.E., 2018. Multi-temporal surveys for microplastic particles enabled by a novel and fast application of SWIR imaging spectroscopy – study of an urban watercourse traversing the city of Berlin, Germany. *Environ. Pollut.* 239, 579–589. <https://doi.org/10.1016/J.ENVPOL.2018.03.097>.
- Sipe, J.M., Bossa, N., Berger, W., von Windheim, N., Gall, K., Wiesner, M.R., 2022. From bottle to microplastics: can we estimate how our plastic products are breaking down? *Sci. Total Environ.* 814, 152460. <https://doi.org/10.1016/J.SCITOTENV.2021.152460>.
- Smith, P.E., Counts, R.C., Clutter, R.I., 1968. Changes in filtering efficiency of plankton nets due to clogging under tow. *ICES (Int. Coun. Explor. Sea) J. Mar. Sci.* 32 (2), 232–248. <https://doi.org/10.1093/icesjms/32.2.232>.
- Strokal, M., Vriend, P., Bak, M.P., Kroeze, C., van Wijnen, J., van Emmerik, T., 2023. River export of macro- and microplastics to seas by sources worldwide. *Nat. Commun.* 14 (1), 1–13, 14(1). <https://www.nature.com/articles/s41467-023-40501-9>.
- Tibbetts, J., Krause, S., Lynch, I., Smith, G.H.S., 2018. Abundance, distribution, and drivers of microplastic contamination in urban river environments. *Water* 10 (11), 1597. 2018, Vol. 10, Page 1597. <https://www.mdpi.com/2073-4441/10/11/1597/html>.
- Wagner, S., Klöckner, P., Stier, B., Römer, M., Seiwert, B., Reemtsma, T., Schmidt, C., 2019. Relationship between discharge and river plastic concentrations in a rural and an urban catchment. *Environ. Sci. Technol.* 53 (17), 10082–10091. Available at: <https://pubs.acs.org/doi/10.1021/acs.est.9b03048>.
- Woodward, J., Li, J., Rothwell, J., Hurlley, R., 2021. Acute riverine microplastic contamination due to avoidable releases of untreated wastewater. *Nat. Sustain.* 4 (9), 793–802, 4(9). <https://www.nature.com/articles/s41893-021-00718-2>.
- Yu, J., Jing, W., Liu, E., Du, S., Cai, H., Du, H., Wang, J., 2024. Sulfonated graphene oxide modified polysulfone-polyamide forward osmosis membrane and its application in fluorine-containing wastewater treatment. *Mater. Chem. Phys.* 313, 128757. <https://doi.org/10.1016/J.MATCHEMPHYS.2023.128757>.
- Zhang, Y., Gao, T., Kang, S., Sillanpää, M., 2019. Importance of atmospheric transport for microplastics deposited in remote areas. *Environ. Pollut.* 254, 112953. Available at: <http://www.sciencedirect.com/science/article/pii/S0269749119325175>.
- Zhu, M., Li, B., Liu, G., 2022. Groundwater risk assessment of abandoned mines based on pressure-state-response—the example of an abandoned mine in southwest China. *Energy Rep.* 8, 10728–10740. <https://doi.org/10.1016/J.EGYR.2022.08.171>.